

ALLOYS OF THE Ti–Si–Sn SYSTEM (TITANIUM CORNER): PHASE EQUILIBRIA, STRUCTURE, AND MECHANICAL PROPERTIES

I. D. Gorna,^{1,2} M. V. Bulanova,¹ K. O. Valuiska,¹
M. D. Bega,¹ O. Yu. Koval',¹ A. V. Kotko,¹
Ya. I. Evich,¹ and S. O. Firstov¹

UDC 669.295:539.22:541.12.03

The joint effect of Si (5, 7, and 10 at.%) and Sn (3–15 at.%) on the structure and mechanical properties of Ti-rich as-cast Ti–Si–Sn alloys is studied. Hypoeutectic alloys with 10 at.% Si are shown to possess the highest level of properties due to a greater volume fraction of the (β^) + Ti_5Si_3 eutectic. It is shown that the dependence of strength and hardness of Ti–Si–Sn alloys on Sn content is nonmonotonic. The properties improve with increasing tin content to 7–10 at.% due to the solid-solution hardening mechanism. The elastic modulus and plasticity of all the alloys decrease with increasing Sn content. The elastic modulus for the alloys with 7–15 at.% Sn almost halves, decreasing to 65–60 GPa. The level of long-term hot hardness of the alloys at different temperatures depends on Si and Sn content. In general, tin additions increase heat resistance of all the alloys studied. The deviation from the dependence for individual alloys results from variation in their phase composition. The mechanical behavior of Ti-rich Ti–Si–Sn alloys depending on Sn content is determined by the formation of the intermetallic Ti_3Sn phase.*

Keywords: titanium alloys, doping, silicon, tin, eutectic, Ti_5Si_3 , Ti_3Sn , structure, mechanical properties.

INTRODUCTION

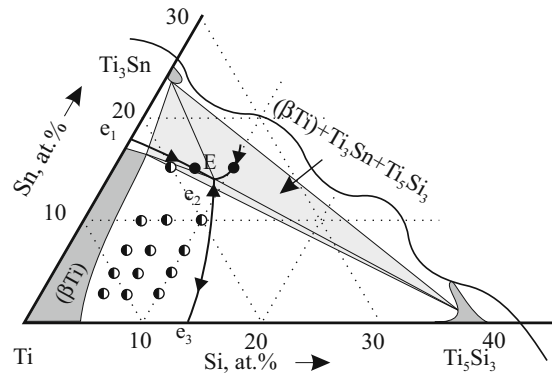
Titanium–silicon eutectic alloys belonging to *in-situ* composites are of special interest among titanium materials with high specific strength and heat resistance [1–5]. The heat resistance of titanium is best increased by α stabilizers, which form substitutional solid solutions with it. Increase in the content of α stabilizers permits additional reinforcement of the titanium solid solution through the formation of ordered particulate intermetallic Ti_3X phases (where X is Al, Ga) and even leads to alloys with an intermetallic matrix. Recent studies of Ti–Si–Ga ternary alloys have shown that heat-resistant titanium alloys with higher hardness and an elastic modulus of about 150 GPa can also be produced [6, 7].

Tin, which is inert to titanium stabilization, forms intermetallic Ti_3Sn with a DO_{19} -type structure isostructural to Ti_3Al and Ti_3Ga . This compound shows uncommon mechanical properties such as high plasticity (>60%) in four-point bending tests (~15%) and abnormally low elastic modulus (~5 GPa) at room temperature [8–10].

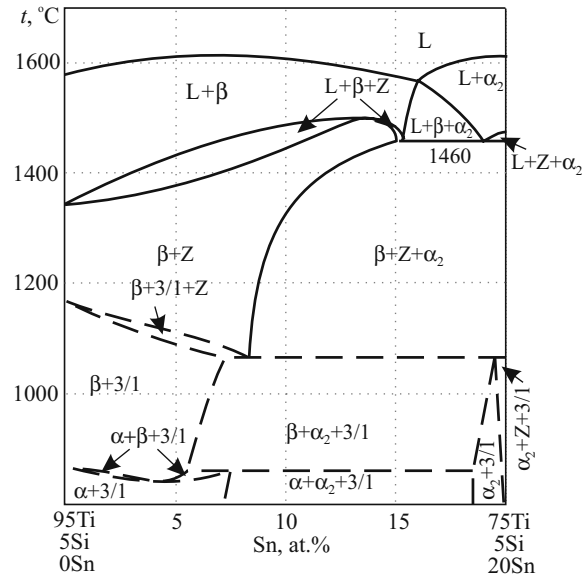
¹Frantsevich Institute for Problems of Materials Science, National Academy of Sciences of Ukraine, Kiev, Ukraine.

²To whom correspondence should be addressed; e-mail: gid@ipms.kiev.ua.

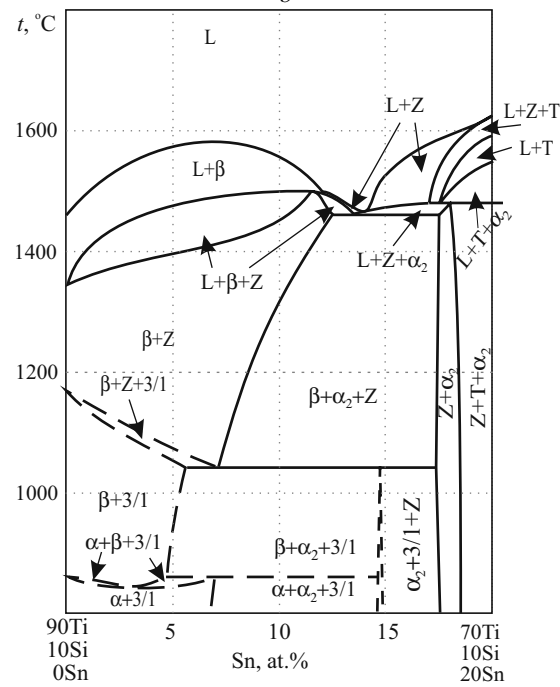
Translated from Poroshkovaya Metallurgiya, Vol. 50, No. 7–8 (480), pp. 87–98, 2011. Original article submitted June 21, 2011.



a



b



c

Fig. 1. Ti-Si-Sn phase diagram [12, 13]: melting diagram (a); vertical sections at 5 (b) and 10 at.% Si (c) isopleths

On the titanium side, the Ti–Sn system has a high-temperature (1600°C) eutectic between β -Ti and Ti_3Sn . There are also extensive regions of solid solutions (β -Ti and α -Ti) in the system.

The peculiar feature of the Ti–Si–Sn phase diagram in the titanium-rich region is the formation of eutectics (e) between Ti_5Si_3 (Z) and β -Ti or Ti_3Sn (α_2) ordered by an intermetallic phase (Fig. 1), which makes *in-situ* composites promising for the development of titanium alloys with special properties, such as low elastic modulus.

The effect of tin on the structure and mechanical properties of Ti–Si alloys has been scarcely studied [11]. The papers [12–14] focus on the phase equilibria in the titanium corner of the Ti–Si–Sn ternary system and its phase diagram (Fig. 1).

The objective of this paper is to examine the joint effect of silicon and tin on the structure and mechanical properties of as-cast Ti–Si–Sn alloys in the titanium-rich region.

EXPERIMENTAL PROCEDURE

Ingots to 100 g in weight were arc-melted from iodide titanium (99.97%), tin (99.99%), and KP-1 silicon on a water-cooled copper hearth in argon additionally purged with molten titanium getter. For homogeneity, the ingots were tilted and melted three times. The composition of the samples was checked using analytical scales. The weight loss after melting was no more than 0.5% and the components were taken in the amounts according to the charge. The structure and phase composition of the alloys were examined with scanning and transmission electron microscopy (SEM and TEM), x-ray diffraction (XRD), and electron microprobe analysis (EMPA).

The mechanical properties (bending strength σ_b and plasticity ε and elastic modulus E) of the samples (3.5 mm \times 5 mm \times 50 mm) were determined in four-point bending tests at room temperature. The Vickers hardness was measured under a 300 N load and the microhardness under a 0.5 N load. The heat resistance was evaluated with a rapid hot hardness test for 1 h under a 10 N load in the temperature range 300–700°C.

RESULTS AND DISCUSSION

We chose three groups of test alloys corresponding to 5, 7, and 10 Si isopleths (at.% here and below) [12, 13]. The tin content of the alloys varied from 3 to 15%. The composition of the samples studied is shown in Fig. 1a. The phase composition of as-cast Ti–Si–Sn alloys and the c/a ratio of lattice parameters of the titanium matrix are summarized in Table 1. Microphotographs of typical structures of as-cast alloys are represented in Fig. 2. We used KP-1 silicon for melting of alloys, so the position of monovariant curves may insignificantly differ from that of the melting diagram (Fig. 1a).

Alloys Ti–5 Si– x Sn. The Ti–5 Si–3 Sn alloy is a polycrystalline solid solution of Si and Sn in an α -Ti matrix, with thin layers of the Ti_5Si_3 silicide phase at its boundaries (Fig. 2a). The hypoeutectic as-cast alloy containing 5% Sn consists of primary β^* (α -Ti) dendrites and a (β^*) + Ti_5Si_3 eutectic (Table 1, Fig. 2b). The hypoeutectic structure of the alloys doped with 7–15% Sn shows three phases: (α -Ti), Ti_5Si_3 , and ordered intermetallic α_2 - Ti_3Sn . According to the vertical section at 5Si isopleth (Fig. 1b) with this tin content, the α_2 - Ti_3Sn phase may precipitate in the Ti matrix as the secondary phase with decreasing temperature as the solubility of tin in β - and α -Ti reduces and the respective phase regions, (β -Ti) + Ti_5Si_3 and (α -Ti) + Ti_5Si_3 , become narrower. Note that the secondary precipitates of Ti_3Sn (the light phase in β^* dendrites of the matrix in Fig. 2b) are fine ((4–12) $\mu\text{m} \times 0.5 \mu\text{m}$) in the alloy containing 10% Sn, and Ti_3Sn grains grow to reach (6–33) $\mu\text{m} \times (0.8–2) \mu\text{m}$ when cooled down at high temperatures in the alloy containing 15% Sn. Hence, this alloy has an unusual structure at first sight (Fig. 2c). In general, one can say that the grains of the secondary Ti_3Sn phase in the Ti–5 Si–15 Sn alloy are almost three to four times coarser than in the alloys containing less tin. It is noteworthy that there are boundaries of β^* dendrites with eutectic colonies, (β^*) + Ti_5Si_3 , against the background of elongated grains of the Ti_3Sn phase (Fig. 2c). The maximum solubility of tin is about 10% in α -Ti according to [15] and about 4% in Ti_5Si_3 [13].

A higher tin amount increases the doping content of the Ti matrix in Ti–5 Si– x Sn alloys and leads to gradual variation in the ratio of α -Ti lattice parameters: from $c/a = 1.5916$ in the alloy containing 3% Sn to $c/a =$

TABLE 1. Phase Composition of As-cast Ti–Si–Sn Alloys and Ratio (c/a) of Lattice Parameters of the Titanium Matrix According to XRD

No.	Alloy, at.%	Phase composition	c/a
1	Ti–5 Si–3 Sn	(α -Ti) ¹⁾ + Ti ₅ Si ₃ (traces)	1.5916
2	Ti–5 Si–5 Sn	(α -Ti) + Ti ₅ Si ₃	1.5943
3	Ti–5 Si–7 Sn	(α -Ti) + Ti ₅ Si ₃	1.5982
4	Ti–5 Si–10 Sn	(α -Ti) + Ti ₃ Sn ²⁾ + Ti ₅ Si ₃	1.5984
5	Ti–5 Si–15 Sn	(α -Ti) + Ti ₃ Sn ²⁾ + Ti ₅ Si ₃	1.5974
6	Ti–7 Si–3 Sn	(α -Ti) + Ti ₅ Si ₃	1.5885
7	Ti–7 Si–5 Sn	(α -Ti) + Ti ₅ Si ₃	1.5947
8	Ti–7 Si–7 Sn	(α -Ti) + Ti ₃ Sn ²⁾ + Ti ₅ Si ₃	1.5978
9	Ti–7 Si–10 Sn	(α -Ti) + Ti ₃ Sn ²⁾ + Ti ₅ Si ₃	1.6054
10	Ti–7 Si–15 Sn	Ti ₃ Sn + (α -Ti)(traces) + Ti ₅ Si ₃	0.8027 ⁴⁾
11	Ti–10 Si–3 Sn	(α -Ti) + Ti ₅ Si ₃	1.5905
12	Ti–10 Si–5 Sn	(α -Ti) + Ti ₅ Si ₃	1.5906
13	Ti–10 Si–7 Sn	(α -Ti) + Ti ₃ Sn ²⁾ + Ti ₅ Si ₃	1.6025
14	Ti–10 Si–10 Sn	Ti ₃ Sn + (α -Ti) + Ti ₅ Si ₃	0.8009 ⁴⁾
15	Ti–10 Si–15 Sn	Ti ₃ Sn + Ti ₅ Si ₃ + (α -Ti) ³⁾	0.7940 ⁴⁾

¹⁾ Note that the β -Ti phase forms during crystallization and then transforms into the α -Ti or (α -Ti) + Ti₃Sn phase during furnace cooling. Transformed β -Ti is denoted by β^* .

²⁾ Secondary precipitate.

³⁾ According to the equilibrium phase diagram (Fig. 1), the phase should be present but was not experimentally observed.

⁴⁾ Value for the Ti₃Sn phase.

= 1.5984 in the alloy containing 10% Sn (Table 1). Interestingly, the c/a ratio decreases to 1.5974 for the Ti–5 Si–15 Sn alloy, which is attributed to lower solubility of tin in titanium when cooled and redistributed among α -Ti and secondary Ti₃Sn precipitates.

Alloys Ti–7 Si– x Sn. The hypoeutectic alloys containing 3–5% Sn consist of two phases: (β^*) and Ti₅Si₃ (Table 1, Fig. 2*d*). The volume fraction of the eutectic component is higher in the alloys containing 7% Si than in those containing 5% Si (Fig. 2*a, d*). The secondary α_2 -Ti₃Sn intermetallic phase (4–12) $\mu\text{m} \times$ (0.5–1) μm in size (the light phase in Fig. 2*e*) forms from primary β^* in the Ti–7 Si–10 Sn alloy (Fig. 2*e*), like in the Ti–5 Si–10 Sn alloy (Fig. 2*b*). In the Ti–7 Si–15 Sn alloy, grains of Ti₃Sn intermetallide are primary and the eutectic consists of the Ti₃Sn and Ti₅Si₃ phases (Fig. 2*f*). Transmission electron microscopy of the fine structure of this alloy (Fig. 3*f*) revealed a domain structure typical of ordered titanium intermetallides [6, 7, 16, 17]. Electron microdiffraction and x-ray diffraction patterns show superlattice reflections, which are evidence of the ordered α_2 -Ti₃Sn phase with $c/a = 0.8027$ (Table 1).

Alloys Ti–10 Si– x Sn. As compared with the two previous groups, alloys containing 3–7% Sn have a hypoeutectic structure with a higher volume fraction of the (β^*) + Ti₅Si₃ eutectic (Fig. 2*g*). According to EMPA, the higher the tin content, the lower the Si content of the titanium matrix (Table 2). At 7% and higher titanium content, the secondary α_2 -Ti₃Sn phase shows up (Fig. 2*h*). When tin content increases to 15 at.%, the alloy matrix becomes intermetallic— α_2 -Ti₃Sn (Fig. 2*i*). The solubility of silicon in α_2 -Ti₃Sn is no more than 1.5 at.% according to [13].

Transmission electron microscopy revealed the most typical features of the fine structure of as-cast Ti–Si–Sn alloys (Fig. 3). As already noted, fine particles of the secondary α_2 -Ti₃Sn phase emerge in the alloys containing

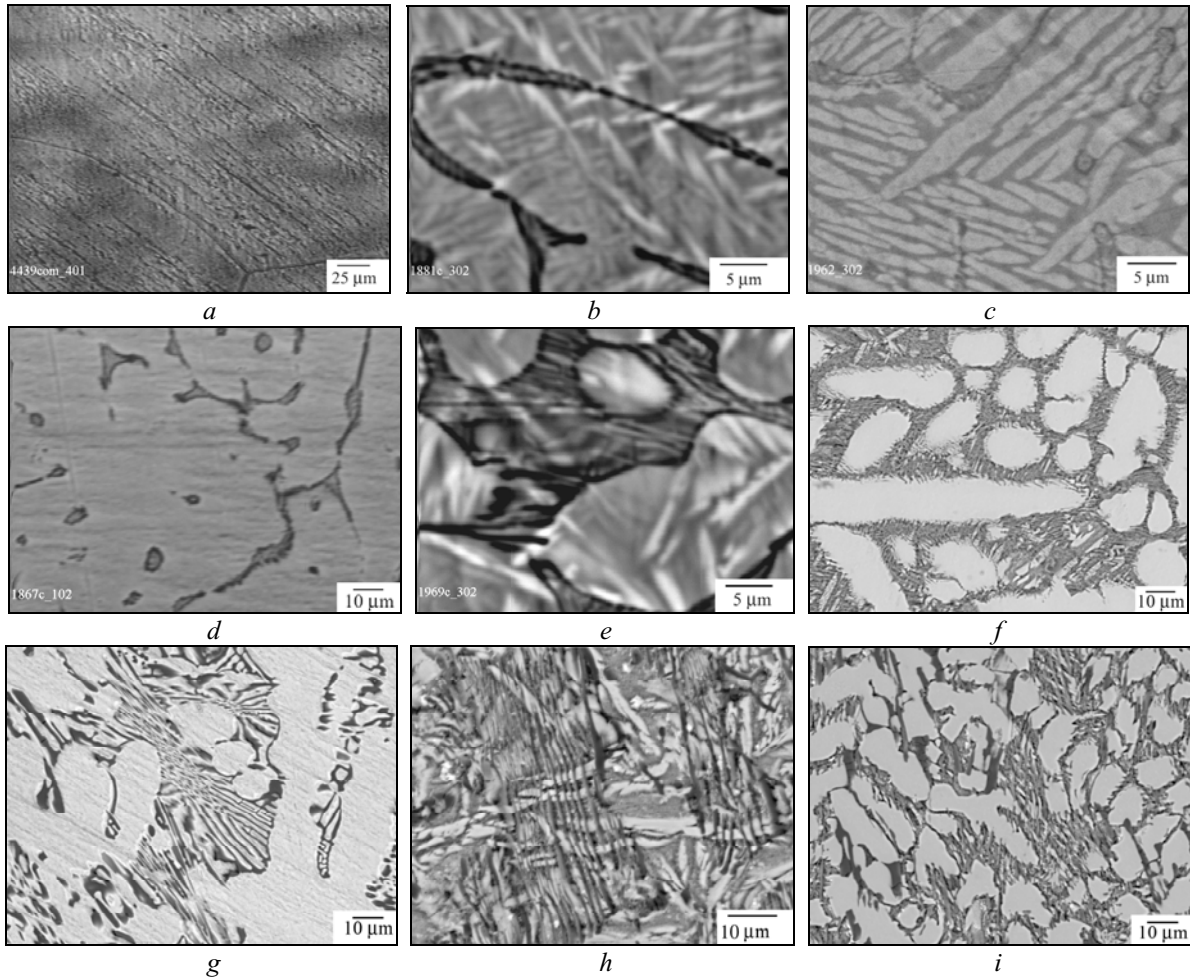


Fig. 2. Microphotographs (SEM) showing the structures of as-cast alloys in the Ti–Si–Sn system: *a*) Ti–5 Si–3 Sn (almost single-phase (α -Ti)); *b*) Ti–5 Si–10 Sn (α -Ti with secondary $Ti_3Sn + e$ ($\beta^* + Z$) precipitates along boundaries of dendrites); *c*) Ti–5 Si–15 Sn (e ($\beta^* + Z$) with secondary Ti_3Sn precipitates); *d*) Ti–7 Si–3 Sn (α -Ti + e ($\beta^* + Z$) at boundaries of dendrites); *e*) Ti–7 Si–10 Sn (α -Ti + e ($\beta^* + Z$) with Ti_3Sn precipitates); *f*) Ti–7 Si–15 Sn ($Ti_3Sn + e$ ($\beta^* + Z$)); *g*) Ti–10 Si–7 Sn (α -Ti + e ($\beta^* + Z$)); *h*) Ti–10 Si–10 Sn (α -Ti with $Ti_3Sn + e$ ($\beta + Z$) precipitates); *i*) Ti–10 Si–15 Sn ($Ti_3Sn + e$ ($\beta + Z$))

5–7% Si and 3–7% Sn in the α -Ti matrix (Fig. 3*a–c*). However, XRD did not identify this phase in these alloys, neither was it observed microstructurally. Such particles are plate-like, ranging from hundreds of nanometers to tens of micrometers in diameter depending on the alloy composition (Fig. 3*b*). At higher tin contents, especially in the

TABLE 2. Amount of Elements in the Matrix of Ti–Si–Sn Alloys According to EMPA

Alloy, at.%	Ti	Si	Sn
Ti–10 Si–3 Sn	93.12	2.75	4.12
Ti–10 Si–5 Sn	90.58	2.45	6.97
Ti–10 Si–7 Sn	87.12	3.15	9.74
Ti–10 Si–10 Sn	87.27	1.57	17.43
Ti–10 Si–15 Sn	74.51	1.61	23.88

alloys with 7 and 10% Si, the dislocation density greatly increases and even low-angle dislocation boundaries show up in the α -Ti matrix, which is evidence of deformation processes in it (Fig. 3*d*). The matrix may deform when the secondary intermetallic α_2 -Ti₃Sn phase forms because the thermal expansion coefficients of the α -Ti and Ti₃Sn phases differ. A domain structure of the ordered intermetallic α_2 -Ti₃Sn phase is observed in the matrix of the Ti–(7–10) Si–15 Sn alloys, which was already mentioned. Figure 3*f* shows some stacking faults against the background of the domain structure of the as-cast Ti–7 Si–15 Sn alloy matrix; they are the typical feature of α_2 -Ti₃Sn, according to the recent studies [8–9].

The Vickers hardness of the three groups of alloys is nonmonotonic as a function of tin content (Fig. 4*a*). The maximum hardness is shown by the alloys containing 10% Si, resulting from the composite hardening mechanism due to a greater amount of the (β^*) + Ti₅Si₃ eutectic (Fig. 1*b, c*). The hardness curves of the alloys containing 10% Si is about 0.5 GPa higher than the two other curves that correspond to 5 and 7% Si and virtually match (Fig. 4*b*). The maximum hardness (4.1–4.3 GPa) is also shown by all alloys doped with 7 and 10% Sn. The higher hardness of the alloys with 7–10% Sn is attributed to the solid-solution hardening mechanism (tin hardens titanium but not as intensively as silicon does) [18, 19]. The hardness of the alloys decreases when tin content increases to 15% since grains of the third phase, titanium stannide (Ti₃Sn), show up regardless of its formation mechanism (Table 1), and its volume fraction gradually increases [13]. As already indicated, this phase demonstrates high plasticity and low elastic modulus at room temperature [8–10].

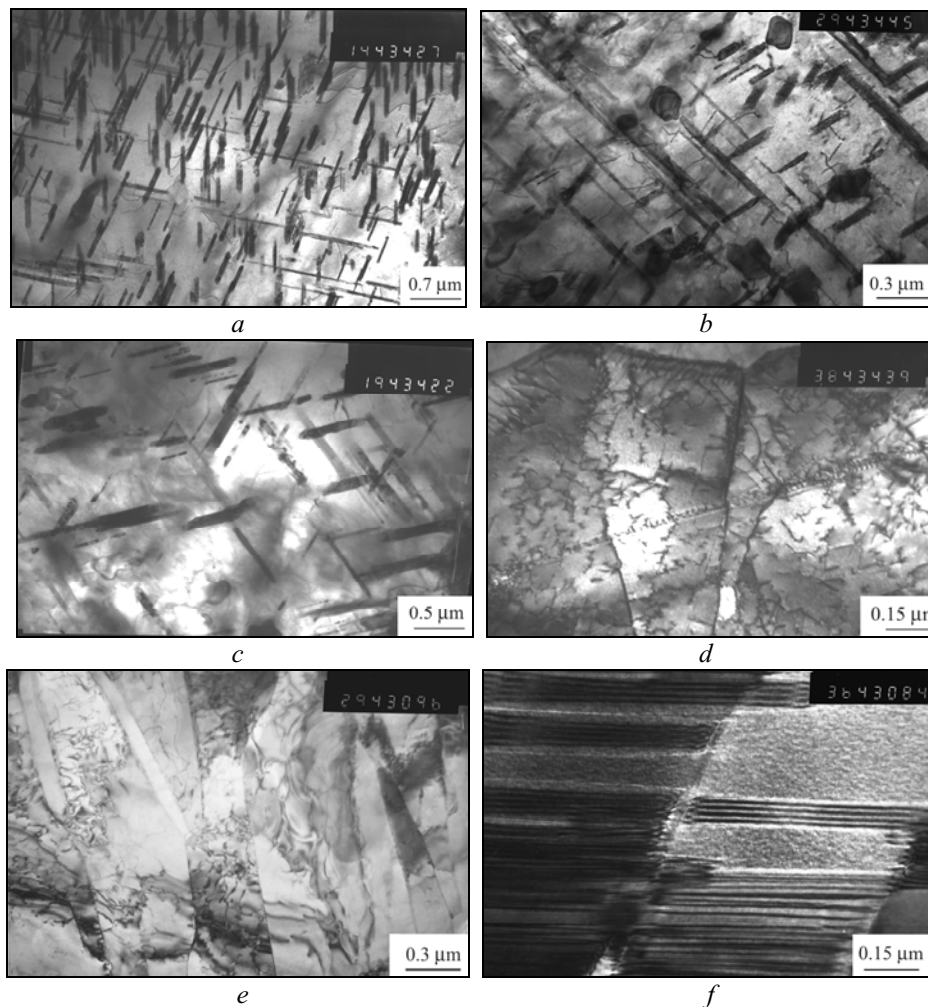


Fig. 3. Microphotographs (TEM) showing the structures of Ti–Si–Sn alloys: Ti–5 Si–3 Sn (*a*); Ti–5 Si–5 Sn (*b*); Ti–7 Si–3 Sn (*c*); Ti–7 Si–7 Sn (*d*); Ti–10 Si–7 Sn (*e*); Ti–7 Si–15 Sn (*f*)

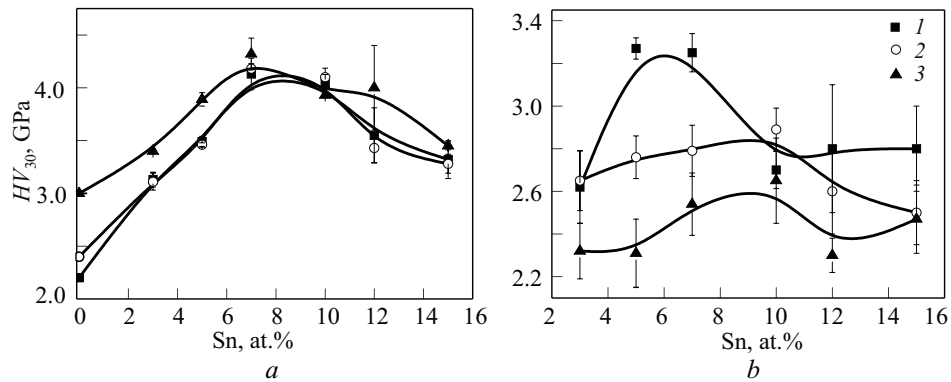


Fig. 4. Tin effect on the Vickers hardness (a) and microhardness (b) of the matrix of as-cast Ti-Si-Sn alloys: 1) Ti-5 Si; 2) Ti-7 Si; 3) Ti-10 Si

Hence, the decrease in hardness is attributed to the mechanical behavior of titanium stannide. Figure 4b shows the microhardness of titanium matrix of the three groups of alloys as a function of tin content. The lowest microhardness is characteristic of the alloys with the maximum silicon content and the highest microhardness of the alloys with the minimum silicon content. This is because the alloys with constant tin content show the lowest silicon content of the matrix if they have the maximum silicon content and vice versa, which is testified by the tie lines in the phase diagram [12, 13]. This dependence for the alloys containing 5% Si is nonmonotonic and has a peak at 5% Sn. The microhardness of the alloys containing 7–10% Si also becomes somewhat higher when Sn content increases to 10%. Transmission electron microscopy of the fine structure of Ti-5 Si-(5–7) Sn alloys, as noted above, revealed superfine plate-like particles of intermetallic Ti_3Sn in the α -Ti matrix (Fig. 3a). These plates in such alloys are secondary precipitates; i.e., the mechanism of solid-solution hardening of the titanium matrix is supplemented by the mechanism of precipitation hardening. The microhardness of the three groups of alloys becomes stable in the composition range 10–15% Sn. Therefore, the microhardness of the matrix is determined by the formation of intermetallic Ti_3Sn and the increase of its volume fraction in the alloys.

Figure 5 shows results from four-point bending tests of as-cast Ti-Si-Sn alloys at room temperature. The typical feature of all three mechanical properties, such as bending strength, elastic modulus, and plasticity, is that they decrease when tin content increases from 7 to 10%. The highest strength is exhibited by the hypoeutectic alloys that contain 7 and 10% Si and are doped with 5–10% Sn (Fig. 5a). The highest plasticity, although it is rather low in general, is demonstrated by the alloy containing 10% Si and 3–10% Sn (Fig. 5b). Further tin doping leads to the α_2 - Ti_3Sn phase, whose volume fraction in the alloys increases and, in turn, determines their brittle fracture.

The mechanical behavior of all alloys is peculiar in that their elastic modulus almost halves (decreasing to 60–65 GPa) at 7–15% Sn (Fig. 5c). This drop in E is primarily due to the intermetallic Ti_3Sn phase present in the

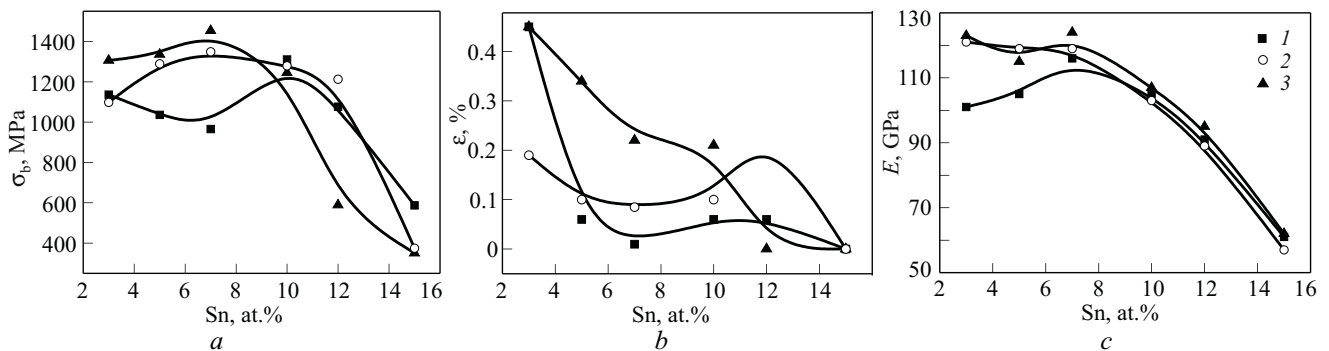


Fig. 5. Tin effect on the mechanical properties of as-cast Ti-Si-Sn alloys: bending strength (a) and plasticity (b); elastic modulus (c); 1) Ti-5 Si; 2) Ti-7 Si; 3) Ti-10 Si

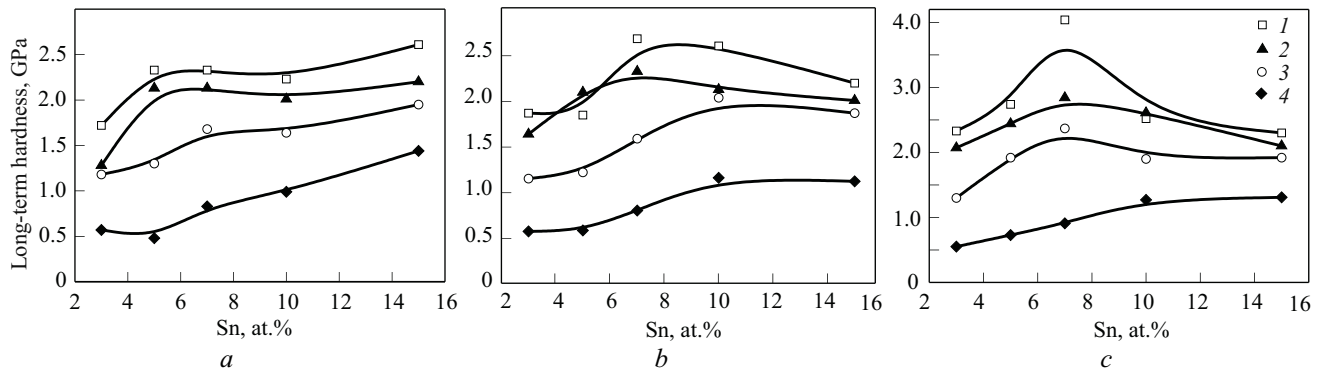


Fig. 6. Tin effect on the temperature dependence of the long-term hot hardness of Ti–5 Si (a), Ti–7 Si (b), Ti–10 Si (c) alloys: 1) 300, 2) 500, 3) 600, 4) 700°C

alloys, which may deform, according to [8–9], through the twinning mechanism, being alternative to the dislocation mechanism.

Evaluation of the long-term hot hardness in the temperature range between 300 and 700°C has shown that the heat resistance of the Ti–Si–Sn alloys generally increases with tin doping (Fig. 6). The long-term hardness of the alloys containing 5% Si increases in the entire temperature range, which is attributed to three major hardening mechanisms: composite (eutectic), solid-solution, and precipitation hardening. Small peaks on the hardness curves at 5–7% Sn in the range 300–500°C result exactly from precipitation hardening due to the formation of superfine grains of the third phase— Ti_3Sn (Fig. 3a–c). The hardness of two other groups of alloys (with 7 and 10% Si) is generally higher at a greater content of the $(\beta^*) + \text{Ti}_5\text{Si}_3$ eutectic as compared with the previous group of alloys and nonmonotonically increases with tin content in the range 300–600°C. The maximum hardening is observed at 7% Sn in the alloys containing 5 and 7% Si in the range 300–500°C and in the alloys containing 10% Si in the range 300–600°C. At 700°C, the maximum heat resistance is shown by the 15% Sn alloys at any silicon content. The Ti–Si binary alloys with the $(\beta^*) + \text{Ti}_5\text{Si}_3$ eutectic are known to demonstrate high heat resistance in the range 500–700°C [1, 2, 4–7, 16, 17]. Comparing binary and ternary alloys, we may state that the peak and subsequent slope of the curves are due to the formation of Ti_3Sn .

However, the coarsening of these precipitates and, hence, the increase in their volume fraction in the alloys at higher tin contents and the acceleration of diffusions processes at higher temperatures change precipitation hardening to composite hardening. This is ascertained by the composition dependence of the long-term hardness of all groups of alloys at 700°C. Note that the composite hardening of alloys in the Ti–Si–Sn system involves hardening due to the $(\beta^* + e(\beta^*) + \text{Ti}_5\text{Si}_3)$ eutectic and the Ti_3Sn phase, whose grains grow through this eutectic (Fig. 2i).

CONCLUSIONS

The joint effect of silicon and tin doping on the structure and mechanical properties of titanium-rich as-cast Ti–Si–Sn alloys has been studied.

It has been established that the hypoeutectic alloys containing 10% Si show the best properties due to a higher volume fraction of the $(\beta^*) + \text{Ti}_5\text{Si}_3$ eutectic.

The dependence of the strength and hardness of as-cast Ti–Si–Sn alloys on tin content is nonmonotonic. The maximum values are shown by the hypoeutectic alloys containing 7 and 10% Si and 7–10% Sn, which may be associated with the boundary solubility of tin in $\alpha\text{-Ti}$ (~10%) and precipitation of the secondary Ti_3Sn phase in the titanium matrix.

When tin content is higher than 7%, the elastic modulus almost halves (~65–60 GPa), which is primarily attributed to the formation of the intermetallic Ti_3Sn phase that may deform, according to [8, 9], through the twinning mechanism, being alternative to the dislocation mechanism.

The plasticity of all alloys decreases with increasing tin content. The highest plasticity is demonstrated by the alloys with 10% Si and 3–10% Sn whose titanium matrix contains minimum silicon, which is evidenced by Auger spectroscopy. Further tin doping leads to the formation of the intermetallic α_2 -Ti₃Sn phase and the increase in its volume fraction in the alloys, determining their brittle fracture.

The long-term hardness of the alloys at different temperatures depends on the joint Si and Sn content. In general, tin doping increases the heat resistance of all alloys. It is shown that the long-term hot hardness (heat resistance) of the alloys containing 5% Si increases with tin content in the temperature range 300–700°C as distinct from the alloys containing 7 and 10% Si, for which this dependence is nonmonotonic with peaks at 7% Sn in the ranges 300–500°C and 300–600°C, respectively. The peak and subsequent slope of the curves are associated with the formation of Ti₃Sn and subsequent increase in its volume fraction. The maximum hardening is observed for the alloys doped with 7% Sn and containing 5 and 7% Si at 300–500°C and for the alloys containing 10% Si at 300–600°C. At 700°C, the heat resistance of all alloys becomes higher when tin content increases to 15%.

ACKNOWLEDGEMENTS

The authors are grateful to S. K. Goltvyanitsa (Rial Ltd., Zaporozhe) for the casting of alloys.

REFERENCES

1. S. Firstov, "Main tendencies in elaboration of materials with high specific strength," in: *Metallic Materials with High Structural Efficiency*, Kluwer Academic Publishers, Dordrecht (2004), pp. 217–228.
2. S. A. Firstov, "Titanium cast irons and titanium steels," *Titan*, **17**, No. 2, 33–37 (2005).
3. M. Bulanova, S. Firstov, and L. Kulak, "Multicomponent Ti–Si-based systems," in: O. Senkov, et al. (eds.), *Metallic Materials with High Structural Efficiency*, Kluwer Academic Publishers, Dordrecht (2004), pp. 217–228.
4. I. D. Gorna, K. O. Gorpenko, O. Yu. Koval', et al., "Structure and physical properties of Ti–Si–X alloys," *Fiz. Khim. Mekh. Mater.*, No. 3, 35–42 (2008).
5. I. D. Gorna, M. V. Bulanova, E. A. Valuiska, et al., "Eutectic alloys of the Ti–Si–X system (X—Al, Ga, Sn, Zr, B): phase equilibria, structure, and properties," in: *Proc. 49th Int. Conf., Current Issues of Strength* [in Russian] (June 14–18, 2010, Kiev, Ukraine), Kiev (2010), p. 180.
6. I. D. Gorna, K. O. Gorpenko, M. D. Bega, et al., "Effect of gallium on the mechanical properties and fracture mechanisms of eutectic alloys in the Ti–Si–Ga system," in: *Interacademic Collection of Scientific Papers on Engineering Mechanics* [in Ukrainian], Lutsk (2007), Issue 20, pp. 106–108.
7. I. D. Gorna, K. O. Gorpenko, M. D. Bega, et al., "Structure and mechanical properties of titanium-rich as-cast Ti–Si–Ga alloys," in: *Electron Microscopy and Strength of Materials* [in Russian], Issue 14, Inst. Probl. Materialoved. NAN Ukrainy, Kiev (2007), pp. 83–88.
8. M. V. Bulanova, Yu. N. Podrezov, Yu. V. Fartushna, et al., "Mechanical behavior of Ti₃Sn intermetallide with different tin contents," in: *Electron Microscopy and Strength of Materials* [in Russian], Issue 17, Inst. Probl. Materialoved. NAN Ukrainy, Kiev (2010), pp. 108–116.
9. I. Yu. Okun', A. V. Kotko, and S. A. Firstov, "Abnormal plasticity in Ti₃Sn intermetallide," in: *Electron Microscopy and Strength of Materials* [in Russian], Issue 14, Inst. Probl. Materialoved. NAN Ukrainy, Kiev (2007), pp. 12–20.
10. O. V. Vdovychenko, M. V. Bulanova, Yu. V. Fartushna, et al., "Dynamic mechanical behavior of intermetallic Ti₃Sn," *Scripta Mater.*, **62**, 758–761 (2010).
11. Jia She and Yongzhong Zhan, "High volume intermetallics reinforced Ti-based composite in situ synthesized from Ti–Si–Sn ternary system," *Mater. Sci. Eng. A*, **528**, No. 10–11, 3871–3875 (2011).
12. M. Bulanova, A. Soroka, P. Zheltov, et al., "Phase equilibria in the Ti-rich corner of the Ti–Si–Sn system," *Z. Metallkd.*, **90**, No. 7, 505–507 (1999).
13. M. Bulanova, L. Tretyachenko, K. Meleshevich, et al., "Influence of tin on the structure and properties of as-cast Ti-rich Ti–Si alloys," *J. Alloys Compd.*, **350**, 164–173 (2003).

14. Zhan Yongzhong, Yang Wenchao, Xu Yanfei, et al., "Experimental phase diagram of the Ti–Si–Sn ternary system at 473 K," *J. Alloys Compd.*, **509**, No. 17, 5269–5273 (2011).
15. C. Colinet, J.-C. Tedenak, and S. G. Fries, "Structural stability of intermetallic phases in the Sn–Ti system," *Calphad*, **33**, 250–259 (2009).
16. I. D. Gorna, M. V. Bulanova, O. I. Bankovsky, et al., "Intermetallic alloys based on α_2 -Ti₃Al reinforced by eutectic silicides Ti₅(Si, Al)₃: phase equilibria, structure, and properties," in: *Proc. 9th Int. Conf. Crystal Chemistry of Intermetallic Compounds* (September 20–24, 2005, Lviv, Ukraine), Lviv (2005), p. 42.
17. I. D. Gorna, O. I. Bankovskii, M. D. Bega, et al., "Structure and properties of intermetallic titanium alloys based on α_2 -Ti₃Al doped with silicon," in: *Electron Microscopy and Strength of Materials* [in Russian], Issue 15, Inst. Probl. Materialoved. NAN Ukrainy, Kiev (2008), pp. 137–145.
18. W. Zwicker, *Titanium and Its Alloys* [Russian translation], Metallurgiya, Moscow (1979), p. 511.
19. E. W. Collings, *The Physical Metallurgy of Titanium Alloys*, ASM International Metals Park, Ohio (1984).